

# Direct determination of the adiabatic ionization energy of NO<sub>2</sub> as measured by guided ion-beam mass spectrometry

D. E. Clemmer and P. B. Armentrout<sup>a)</sup>

Department of Chemistry, University of Utah, Salt Lake City, Utah 84112

(Received 16 April 1992; accepted 4 May 1992)

The adiabatic ionization energy (IE) of NO<sub>2</sub> is measured to be  $9.60 \pm 0.03$  eV by studying the charge-transfer reactions of Zn<sup>+</sup>, NO<sup>+</sup>, and CH<sub>3</sub>I<sup>+</sup> with NO<sub>2</sub> and those of NO<sub>2</sub><sup>+</sup> with  $\alpha,\alpha,\alpha$ -trifluorotoluene and CH<sub>3</sub>I using guided ion-beam mass spectrometry. This value confirms the accuracy of a very precise spectroscopic value measured by Haber *et al.* [J. Chem. Phys. **144**, 58 (1988)] and Tanaka and Jursa [J. Chem. Phys. **36**, 2493 (1962)], IE(NO<sub>2</sub>) =  $9.586 \pm 0.002$  eV, but is much lower than many other measurements that are limited by very unfavorable Franck–Condon factors. The mechanism that allows the charge-transfer reactions to occur at the thermodynamic limit is discussed by examining qualitative potential-energy surfaces for the charge-transfer processes.

## I. INTRODUCTION

During the past 60 years the value for the ionization energy (IE) of nitrogen dioxide has been measured many times by electron impact,<sup>1–7</sup> photoionization,<sup>8–12</sup> photoelectron,<sup>13–17</sup> spectroscopic,<sup>18–20</sup> and chemical techniques.<sup>21,22</sup> The lack of agreement between these measurements, listed in Table I, is surprising since NO<sub>2</sub> is a stable three-atom molecule and normally all of the aforementioned techniques can accurately measure IE's for such species. The difficulty in measuring the adiabatic IE of NO<sub>2</sub> is due to the radical geometry change in going from NO<sub>2</sub> (having an equilibrium bond angle of 134°) (Ref. 23) to NO<sub>2</sub><sup>+</sup> (a linear ion that is isoelectronic with CO<sub>2</sub>). Thus, the vanishingly small Franck–Condon factors that couple the ground states of neutral and ionic NO<sub>2</sub> make the adiabatic ionization transition virtually impossible to access.

The earliest measurements of IE(NO<sub>2</sub>) generally yielded values, Table I, close to the vertical IE of  $\sim 11$  eV.<sup>24</sup> Of the early work, the photoionization study of Dibeler *et al.*,<sup>11</sup> which agreed with earlier values of Nakayama *et al.*<sup>9</sup> and Frost *et al.*,<sup>10</sup> seemed to provide the most accurate assessment of the adiabatic IE,  $9.75 \pm 0.01$  eV. This value is often cited.<sup>25</sup> This comfortable state of affairs was disrupted in 1968 by the photoelectron study of Natalis and Collin,<sup>14</sup> who suggested that IE(NO<sub>2</sub>) was 8.8 eV based on an extrapolation of vibrational features. Reasonably definitive evidence that IE(NO<sub>2</sub>) could not be this low was provided Fehsenfeld, Ferguson, and Mosesman (FFM) in 1969.<sup>21</sup> They found that the charge-transfer reaction of NO<sub>2</sub><sup>+</sup> + NO occurs efficiently at thermal energies, suggesting that IE(NO<sub>2</sub>)  $\geq$  IE(NO) =  $9.264\ 36 + 0.000\ 06$  eV.<sup>25</sup> In the study of FFM, NO<sub>2</sub><sup>+</sup> was produced by charge transfer from O<sub>2</sub><sup>+</sup>, and a buffer gas of Ar was used to ensure that the NO<sub>2</sub><sup>+</sup> ions were thermalized. In 1970, Brundle<sup>13</sup> suggested that the lowest value for IE(NO<sub>2</sub>) that could be reasonably determined by photoelectron spectroscopy is 10.0 eV and that the anomalously low value given by Natalis and Collin was a

result of NO contamination. Upon reinvestigation of their system, Natalis, Delwiche, and Collin agreed that the 8.8 eV value was based on vibrational features due to an NO contaminant in the NO<sub>2</sub> sample.<sup>16</sup>

In 1973, Killgoar *et al.*<sup>12</sup> carefully examined the photoionization efficiency for NO<sub>2</sub> in its threshold region between 1295–1225 Å (9.57–10.12 eV). To attempt to overcome the Franck–Condon overlap problem, they relied on autoionization processes. They obtained IE(NO<sub>2</sub>)  $\leq 9.62$  eV from the lowest-energy peak observed coupled with a vibrational progression from larger, more easily distinguished peaks at higher photon energies. Many of the peaks in the photoionization efficiency curve corresponded well with optically observed peaks in the vacuum ultraviolet absorption measurements of Tanaka and Jursa;<sup>26</sup> however, Killgoar *et al.* did not observe an ionization peak at 1293 Å (9.589 eV) which Tanaka and Jursa had assigned as the  $\nu = 0$  level of one member of the autoionizing Rydberg state. This could either be because this level is below IE(NO<sub>2</sub>) or because the autoionization rate at this energy is too slow to allow easy observation of an ion signal.

In 1978, Ausloos and Lias<sup>22</sup> (AL) examined the reaction of NO<sub>2</sub><sup>+</sup> +  $\alpha,\alpha,\alpha$ -trifluorotoluene in an ion cyclotron resonance (ICR) mass spectrometer. Here, NO<sub>2</sub><sup>+</sup> was produced by electron impact ionization of ethyl nitrate at an electron energy of 25 eV. They found that the thermal rate constant for this charge-transfer reaction was  $(6.9 \pm 0.4) \times 10^{-10}$  cm<sup>3</sup>/s, a result that has been interpreted<sup>25,27</sup> to indicate that IE(NO<sub>2</sub>) exceeds IE(C<sub>6</sub>H<sub>5</sub>CF<sub>3</sub>) =  $9.685 + 0.004$  eV (Ref. 25) and, hence, that the photoionization value of IE(NO<sub>2</sub>) =  $9.75 \pm 0.01$  eV must be correct, rather than a value near 9.6 eV.

The most recent report of IE(NO<sub>2</sub>) was given by Grant and co-workers in 1988.<sup>20</sup> In an elaborate three-color experiment, two photons were used to excite the bent neutral molecule to low-lying rovibrational states of a linear Rydberg state,<sup>28,29</sup> and a third photon was used to ionize the molecule. Utilizing the linear Rydberg state in this manner bypassed the Franck–Condon constraints encountered by more conventional one-photon spectroscopic and electron

<sup>a)</sup> Camille and Henry Dreyfus Teacher-Scholar, 1987–1992.

TABLE I. Reported values for the first or adiabatic ionization energy of NO<sub>2</sub>.

| IE(NO <sub>2</sub> ) (eV) | Reference | Technique <sup>a</sup>     | Year |
|---------------------------|-----------|----------------------------|------|
| 11.0 ± 1.1                | 1         | EI                         | 1930 |
| 12.3 ± 0.2                | 18        | spec.                      | 1941 |
| 9.91                      | 2         | EI (indirect) <sup>b</sup> | 1955 |
| 11.3 ± 0.4                | 8         | PI                         | 1959 |
| 9.78 ± 0.05               | 9         | PI                         | 1959 |
| 11.27 ± 0.19              | 4         | EI                         | 1961 |
| ≤9.93                     | 5         | EI (indirect) <sup>b</sup> | 1962 |
| 9.80 ± 0.05               | 10        | PI                         | 1962 |
| 9.589                     | 26        | spec.                      | 1962 |
| 10.97                     | 17        | PE                         | 1966 |
| 10.75 ± 0.01              | 11        | PI                         | 1967 |
| 8.8                       | 14        | PE                         | 1968 |
| ≥9.25                     | 21        | chem.                      | 1969 |
| 10.0                      | 13        | PE                         | 1970 |
| ≤9.62                     | 12        | PI                         | 1973 |
| ≥9.685                    | 22        | chem.                      | 1978 |
| 9.586 ± 0.002             | 20        | spec.                      | 1988 |
| 9.60 ± 0.03               | This work | chem.                      | 1992 |

<sup>a</sup>EI represents electron impact, PE the photoelectron spectroscopy, PI the photoionization, spec. the spectroscopy, and chem. the chemical techniques.

<sup>b</sup>These values are considered indirect since they are derived by measuring the appearance energy of NO<sub>2</sub><sup>+</sup> from EI of nitromethane (Ref. 2) and ethyl nitrate (Ref. 5).

impact ionization techniques. Their value of IE(NO<sub>2</sub>) = 9.586 ± 0.002 eV agrees with the limit of Killgoar *et al.*<sup>12</sup> and corresponds exactly with the 1293 Å line observed by Tanaka and Jursa.<sup>26</sup> It disagrees, however, with the value from AL and most previous measurements. While the determination of this threshold is relatively straightforward (although experimentally complex), it is possible that the ionization limit observed corresponds to a vibrationally excited state of the NO<sub>2</sub><sup>+</sup> ion.

The primary purpose of the present work is to measure the ionization energy of NO<sub>2</sub> by using guided ion-beam mass spectrometry and to resolve some of the discrepancies in the literature. To do this, we have studied five charge-transfer reactions: Zn<sup>+</sup>, NO<sup>+</sup>, and CH<sub>3</sub>I<sup>+</sup> + NO<sub>2</sub> and NO<sub>2</sub><sup>+</sup> + α,α,α-trifluorotoluene, and CH<sub>3</sub>I. In cases where the reactions are endothermic, a determination of the collision energy necessary to induce charge-transfer allows us to measure a value for IE(NO<sub>2</sub>). We also undertook this work as a challenging model problem to see if guided ion-beam techniques can be used to measure accurate IE's for molecules that undergo radical geometry changes upon removal of an electron. This question is particularly interesting since translational, vibrational, and rotational energy is being used to drive a process that is intrinsically electronic, a violation of the Born–Oppenheimer principle.

## II. EXPERIMENT

### A. General

The guided ion-beam instrument used for these experiments has been described in detail previously.<sup>30</sup> Ions are created as described later, extracted from the source, accel-

erated, and focused into a magnetic sector momentum analyzer for mass analysis. The mass-selected ions are slowed to a desired kinetic energy and focused into an octopole ion guide that radially traps the ions. The octopole passes through a static gas cell containing the neutral reagent (either NO<sub>2</sub>, CH<sub>3</sub>I, or α,α,α-trifluorotoluene).<sup>31</sup> Pressures within the cell are kept low (between 0.02 and 0.18 mTorr) so that multiple ion-molecule collisions are improbable. Product and unreacted beam ions are contained in the guide until they drift out of the gas cell where they are focused into a quadrupole mass filter for mass analysis and then detected. Absolute cross sections are calculated from ion intensities as described before.<sup>30</sup> Uncertainties in cross sections are estimated to be ± 20%.

Laboratory ion energies are related to center-of-mass (c.m.) frame energies by  $E_{c.m.} = E_{lab} m / (M + m)$ , where  $M$  and  $m$  are the ion and neutral reactant masses, respectively. Below ~0.3 eV lab, energies are corrected for truncation of the ion-beam energy distribution as described previously.<sup>30</sup> Absolute energy scale uncertainties are ± 0.05 eV lab. Two effects broaden the data: the ion energy spread, which is independent of energy and has a full width at half maximum (FWHM) of 0.3 to 0.7 eV lab, and thermal motion of the neutral gas. The latter effect, referred to as Doppler broadening, can be calculated according to an equation given by Chantry,<sup>32</sup> and in these experiments ranges from 0.2  $E_{c.m.}^{1/2}$  to 0.5  $E_{c.m.}^{1/2}$ .<sup>33</sup>

### B. Ion sources

Ions were produced in a flow tube source.<sup>34</sup> Here, a microwave discharge forms helium ions and metastables that interact downstream with the reagent gas, either NO, NO<sub>2</sub>, or CH<sub>3</sub>I, to form the parent ions through charge transfer or Penning ionization. The flow tube length was 100 cm and the He flow rate was ~6000 standard cm<sup>3</sup>/s. Under these conditions, ions undergo ~10<sup>5</sup> collisions with the He buffer gas before leaving the flow tube. Zn<sup>+</sup> ions were produced in the flow tube by using a dc-discharge source, described in detail elsewhere.<sup>35</sup> Briefly, Ar is added to the He flow (up to 10%) and ionized in a high voltage dc discharge where the cathode is made of zinc. Argon ions sputter the cathode to produce the atomic metal ions.

### C. Ion state distributions

Since the initial ionization process in these sources is a highly energetic process, the possibility that the ions have significant populations of excited states must be considered. It seems unlikely that excited *electronic* states of the molecular ions, NO<sup>+</sup>, NO<sub>2</sub><sup>+</sup>, and CH<sub>3</sub>I<sup>+</sup> are present since radiative emission can cool any states having lifetimes shorter than milliseconds and metastable states are exposed to electron collisions in the weak plasma and ~10<sup>5</sup> collisions with He. Such conditions do not guarantee that there are no electronically excited states,<sup>36,37</sup> but the present experiments show no obvious indication of the presence of such states. We have verified that the present results correspond to ground-state Zn<sup>+</sup> (<sup>2</sup>S) by finding comparable results for

action of NO<sub>2</sub> with Zn<sup>+</sup> formed in the flow tube and formed by low-energy electron impact (< 15 eV), a source known to produce only Zn<sup>+</sup> (<sup>2</sup>S).<sup>38,39</sup>

The presence of vibrationally excited states in our molecular ion beams is more difficult to ascertain quantitatively. Previous work in our laboratory indicates that ions produced in the flow tube source [these include O<sub>2</sub><sup>+</sup> (Ref. 40), N<sub>2</sub><sup>+</sup> (Ref. 41), N<sub>4</sub><sup>+</sup> (Ref. 42), Fe(CO)<sub>x</sub><sup>+</sup> (*x* = 1–5) (Ref. 35), and SF<sub>x</sub><sup>+</sup> (*x* = 1–5) (Ref. 36)] are thermalized to 300 K. As discussed further later, the present results for reactions of NO<sup>+</sup> and CH<sub>3</sub>I<sup>+</sup> are consistent with ions that are also thermalized with respect to vibrational and rotational states. A Maxwell–Boltzmann distribution at 300 K predicts that vibrational excited states are virtually unpopulated in the NO<sup>+</sup> beam (the fraction is  $\sim 2 \times 10^{-5}$ ) and comprise about 8% of the CH<sub>3</sub>I<sup>+</sup> beam, due mainly to population of the lowest-frequency mode<sup>43</sup> at 570 cm<sup>-1</sup> (*v* = 1 and 2 of this mode comprise  $\sim 5\%$  and  $\sim 2\%$  of the beam, respectively).

In the case of NO<sub>2</sub><sup>+</sup>, the behavior observed is more complex. A Maxwell–Boltzmann distribution at 300 K predicts that excited vibrational states comprise about 10% of the beam (mainly due to the *v* = 1 state of the lowest-frequency mode at 614.5 cm<sup>-1</sup>).<sup>44</sup> As discussed further in Sec. III, when NO<sub>2</sub><sup>+</sup> is formed as described earlier (in a flow containing only He gas), the results clearly indicate the presence of excited ions. Addition of CO<sub>2</sub> to the He flow gas at a flow rate of 500 sccm was found to substantially reduce this population of excited states as observed by changes in the reaction cross sections. Further addition of CO<sub>2</sub> in 500 sccm increments to a maximum of 2000 sccm did not result in any further changes in the results nor did addition of other buffer gases such as Ar and N<sub>2</sub>. These results are consistent with formation of thermalized (300 K) NO<sub>2</sub><sup>+</sup> ions under these latter conditions.

#### D. Charge-transfer threshold analyses

The adiabatic IE of a molecule is by nature a 0 K value. In order to accurately measure this quantity in processes involving reactants and products at other temperatures, the contributions of all sources of energy to the ionization process must be accounted for. For systems at equilibrium, this has been discussed previously.<sup>45</sup> In the present work, charge-transfer occurs via a nonequilibrium process in which the internal energy of the reactants is characterized by the temperatures of the reactant sources while the internal energy of each product depends on how the total energy is partitioned. Recent work in our laboratories<sup>35,36</sup> has suggested that the most reasonable assumption regarding the measurement of the energy thresholds for endothermic dissociation reactions is that all available translational and internal energy of the reactants is available to drive the reaction and that products at threshold are formed with no excess energy, i.e., at 0 K. This assumption will be explicitly tested in the present system since it is not obvious that nuclear motion (vibrational, rotational, and translational ener-

gy) will necessarily couple directly to facilitate the electronic transition involved in charge transfer.

Theory<sup>46,47</sup> and experiment<sup>48–51</sup> show that cross sections for endothermic reactions can be modeled by

$$\alpha = \sigma_0 \sum_{g_i} (E + E_i - E_0)^n / E \quad (1)$$

which involves a summation over the reactants' internal states *i* having energies *E<sub>i</sub>* and relative populations of *g<sub>i</sub>*, where  $\sum_{g_i} = 1$ . *E* is the relative kinetic energy, *n* is an adjustable parameter, and *E<sub>0</sub>* is the 0 K threshold energy.  $\sigma_0$  is a scaling factor and we assume that the relative reactivity of each state is the same, i.e.,  $\sigma_0$  and *n* are the same for all states *i*. Before comparison with the experimental data, this model is convoluted with the neutral and ion kinetic-energy distributions as described previously.<sup>30</sup> The  $\sigma_0$ , *n*, and *E<sub>0</sub>* parameters are then optimized by using a nonlinear least-squares analysis to give the best reproduction of the data. Error limits for *E<sub>0</sub>* are calculated from the range of threshold values obtained for different data sets and the error in the absolute energy scale.

In previous work,<sup>35</sup> we have introduced a method to explicitly include the vibrational states in the summation of Eq. (1). In the present study we extend this method to explicitly include both vibrational and rotational states of both reactants. The relative electronic and vibrational state populations and energy levels for inclusion in Eq. (1) can be derived as discussed previously.<sup>35</sup> The rotational and rovibrational state populations and energies are calculated as a Maxwell–Boltzmann distribution at 300 K where the Beyer–Swinehart algorithm<sup>52</sup> is used to calculate the rotational and rovibrational density of states of the reactants. The resulting distribution of energies and modes is then divided into a maximum of 32 bins, and the bin populations are used as the weighting factors *g<sub>i</sub>* in Eq. (1). The bin sizes are chosen to be as small as possible (5–30 cm<sup>-1</sup>) while including at least 90% of the total available internal energy. They are also chosen to maintain an average internal energy within 0.01 eV of the average of the model frequencies used, which is calculated exactly by statistical mechanics for comparison.

### III. RESULTS AND DISCUSSION

#### A. NO<sub>2</sub><sup>+</sup> + C<sub>6</sub>H<sub>5</sub>CF<sub>3</sub>

Figure 1 shows the charge-transfer (CT) cross section for interaction of NO<sub>2</sub><sup>+</sup> with  $\alpha,\alpha,\alpha$ -trifluorotoluene:



Results are shown for NO<sub>2</sub><sup>+</sup> ions produced in a pure flow of He, and when CO<sub>2</sub> buffer gas is added to the flow at 500 sccm. Under the former flow conditions, reaction (2) has a large cross section at the lowest kinetic energies that decreases as the energy is increased until  $\sim 0.8$  eV. This behavior suggests an exothermic reaction, consistent with the observations of Ausloos and Lias<sup>22</sup> who produced NO<sub>2</sub><sup>+</sup> by electron impact ionization of ethyl nitrate (C<sub>5</sub>H<sub>5</sub>ONO<sub>2</sub>) using 25 eV electrons and did nothing to quench the ions before reaction. In contrast, when CO<sub>2</sub> is added to the flow, the

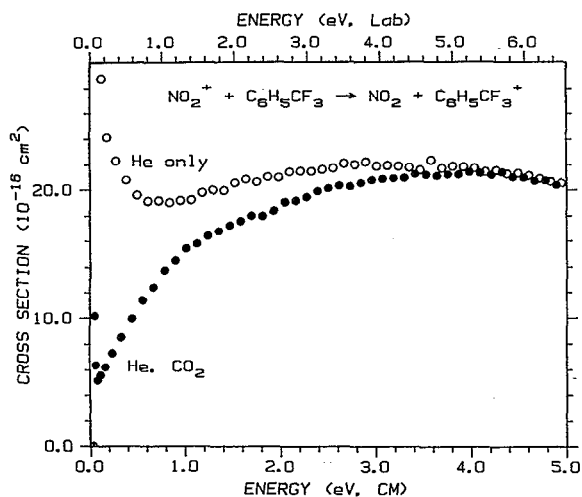
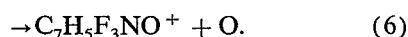
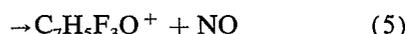
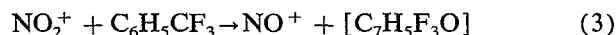


FIG. 1. Cross sections for formation of  $C_6H_5CF_3^+$  from the reaction of  $NO_2^+$  with  $\alpha,\alpha,\alpha$ -trifluorotoluene as a function of kinetic energy in the center-of-mass frame (lower axis) and laboratory frame (upper axis). Open circles show the reaction cross section when  $NO_2^+$  is produced in a flow of helium. Solid circles show the cross section obtained when  $CO_2$  is added to the helium flow.

cross section for reaction (2) changes appreciably such that it no longer behaves like an exothermic reaction, Fig. 1. This change in behavior clearly indicates that the exothermic reactivity observed is due to excited  $NO_2^+$  ions. It seems likely that this excitation is vibrational since  $CO_2$  and  $NO_2^+$  are isoelectronic and have nearly resonant vibrational frequencies. Thus,  $CO_2$  should be an efficient quencher of vibrationally excited  $NO_2^+$ .

These observations lead to two important results. First, we can discard the limit of  $IE(NO_2) > IE(C_6H_5CF_3) = 9.695$  eV suggested by AL, and replace it with an upper limit for  $IE(NO_2)$  of  $\leq 9.695$  eV. Second, it is clear that internal energy can couple to facilitate the charge transfer. Thus, in order to measure an accurate IE from a CT reaction, the internal energy of the reactants must be taken into account.

We do not model the cross section for reaction (2) to obtain a threshold since this analysis is complicated by competition between the CT reaction channel and several additional products formed at low energies in the exothermic reactions (3)–(6):

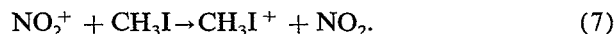


At low energies ( $\sim 0.06$  eV), these reactions are roughly 67%, 3%, 9%, and 19%, respectively, of the total reaction cross section of  $386 \text{ \AA}^2$ , somewhat larger than what we calculate for the Langevin–Gioumousis–Stevenson<sup>53</sup> (LGS) collision cross section at our lowest energies.<sup>54</sup> Formation of  $C_6H_5CF_3^+$ ,  $C_6H_5CF_2^+$ , and  $C_6H_5CF_3O^+$  ions were also observed in the ICR study of AL; however, they do not men-

tion reactions (3) and (6), although it is not clear that an exhaustive search for all products was performed.

## B. $NO_2^+ + CH_3I \rightleftharpoons CH_3I^+ + NO_2$

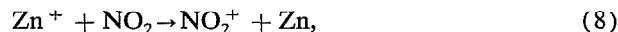
Figure 2 shows the cross sections for charge transfer between  $NO_2^+$  (produced using a flow that contains  $CO_2$ ) and  $CH_3I$ :



The magnitude of  $\sigma(CH_3I^+)$  is large and comparable to total collision cross sections calculated by the LGS (Ref. 53) and locked-dipole (LD) (Ref. 55) models. This shows that the reaction occurs exothermically for most if not all states of  $NO_2^+$  in the beam and that  $IE(NO_2) > IE(CH_3I) = 9.534 \pm 0.005$  eV.<sup>56</sup> This limit is confirmed by the observation that the reverse of reaction (7) is slightly endothermic, Fig. 2. A more detailed evaluation of the endothermicity of this reaction using Eq. (1) was attempted but the shape of the reaction cross section is difficult to analyze definitively. We note that the cross section can be reproduced by Eq. (1) using thresholds that are consistent with values predicted from the thermochemistry determined later from the  $Zn^+ + NO_2$  and  $NO^+ + NO_2$  systems.

## C. $Zn^+$ and $NO^+ + NO_2$

Our results for reactions (2) and (7) establish that  $9.534 \text{ eV} < IE(NO_2) < 9.695 \text{ eV}$ . In order to obtain a more precise value, we studied the CT reactions of  $Zn^+$  and  $NO^+$  with  $NO_2$ :



These ionic reactants were chosen for three reasons. First, the IE's of Zn and NO are  $9.39420 + 0.00002$  eV (Ref. 57)

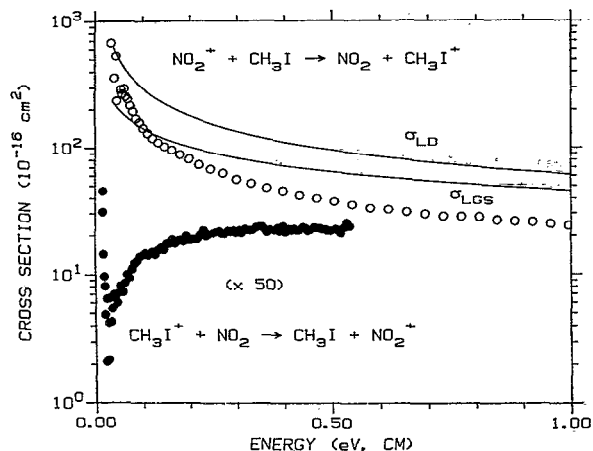


FIG. 2. Cross sections for formation of  $CH_3I^+$  from the reaction of  $NO_2^+ + CH_3I$  (open circles) and formation of  $NO_2^+$  from the reaction of  $CH_3I^+ + NO_2$  (solid circles multiplied by a factor of 50) as a function of kinetic energy in the center-of-mass frame (lower axis) and laboratory frame (upper axis). The solid lines show the LGS and LD theoretical collision cross sections.

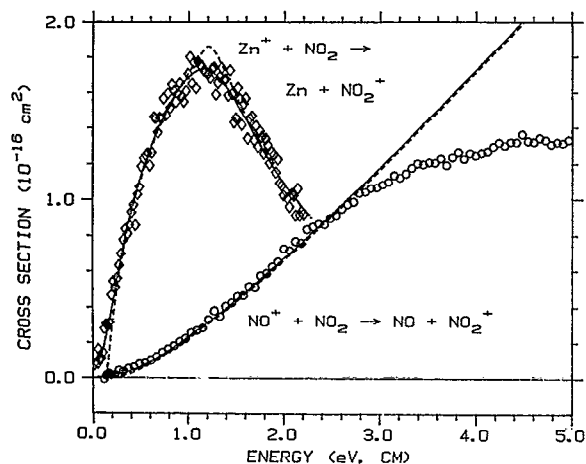


FIG. 3. Cross sections for formation of NO<sub>2</sub><sup>+</sup> from the reactions of Zn<sup>+</sup> + NO<sub>2</sub> (open diamonds) and NO<sup>+</sup> + NO<sub>2</sub> (solid circles) as a function of kinetic energy in the center-of-mass frame (lower axis) and laboratory frame (upper axis). The solid lines are Eq. (1) with the parameters in Table II convoluted over the experimental kinetic-energy distribution, while the dashed lines are the unconvoluted models.

and  $9.264\ 36 \pm 0.000\ 06$  eV (Ref. 25), respectively, such that reactions (8) and (9) are near thermoneutral but definitely endothermic. Second, there are no reactions that compete with reactions (8) and (9) in the threshold region.<sup>58</sup> Third, these ionic reactants minimize the number of internal degrees of freedom. At 300 K, the average energy stored in vibrational modes ( $E_{\text{vib}}$ ) and rotational energy ( $E_{\text{rot}}$ ) of NO<sub>2</sub> is 0.003 and  $3kT/2 = 0.039$  eV, respectively. For NO<sup>+</sup>,  $E_{\text{vib}}$  is less than 0.0001 eV and  $E_{\text{rot}} = kT = 0.026$  eV, and atomic Zn<sup>+</sup> contains no vibrational or rotational energy.

The cross sections for reactions (8) and (9) are shown in Fig. 3. The thresholds for these cross sections are analyzed by using Eq. (1) and the optimized parameters are given in Table II. The thresholds of  $0.21 \pm 0.03$  and  $0.28 \pm 0.11$  eV for the Zn<sup>+</sup> and NO<sup>+</sup> reactions, respectively, are believed to be those appropriate for 0 K products since their derivation explicitly includes contributions from the distributions of translational, vibrational, and rotational states of both reactants. When these thresholds are combined with the IE's of Zn and NO, we obtain values for IE(NO<sub>2</sub>) of  $9.60 \pm 0.03$  and  $9.55 \pm 0.11$  eV, respectively. We take our most reliable value to be the weighted average of these two results, IE(NO<sub>2</sub>) =  $9.60 \pm 0.03$  eV. This value falls within the limits set by our results for reactions (2) and (7) and is in good agreement with the results of Killgoar *et al.*,<sup>12</sup> Tanaka and Jursa,<sup>26</sup> and Grant and co-workers.<sup>20</sup>

We note that if the internal energy of the reactants was not included in the final determination of the thresholds for reactions (8) and (9), the values for IE(NO<sub>2</sub>) that would have been obtained are  $9.56 \pm 0.03$  and  $9.48 \pm 0.11$  eV, respectively. While both values are still within experimental error of the 9.586 eV value from the literature, the agreement is certainly less satisfying than that obtained for the values that include the internal energy. While these results do not definitively show whether internal energy assists the charge-

TABLE II. Parameters of Eq. (1) used to model reaction cross sections.

| System                            | $\sigma_0$      | $E_0$ (eV)      | $n$           |
|-----------------------------------|-----------------|-----------------|---------------|
| Zn <sup>+</sup> + NO <sub>2</sub> | $1.9 \pm 0.4$   | $0.21 \pm 0.03$ | $1.2 \pm 0.1$ |
| NO <sup>+</sup> + NO <sub>2</sub> | $0.22 \pm 0.06$ | $0.28 \pm 0.11$ | $2.2 \pm 0.1$ |

transfer reactions (8) or (9), when coupled with our observations for reaction (2), the present study does suggest that the contribution of internal energy needs to be carefully considered when evaluating the thermochemistry of charge transfer reactions.

#### D. Potential-energy surfaces

The ionization mechanism that allows nearly resonant endothermic charge-transfer reactions to produce vibrationless NO<sub>2</sub><sup>+</sup> can be understood in terms of qualitative potential-energy surfaces. We discuss these surfaces in detail for the Zn<sup>+</sup> + NO<sub>2</sub> reaction since this system contains the fewest atoms; however, the ideas should be general to all of the systems studied here. Of course, we need to consider both the interaction of Zn<sup>+</sup> (<sup>2</sup>S) with NO<sub>2</sub> (<sup>2</sup>A<sub>1</sub>) and Zn(<sup>1</sup>S) with NO<sub>2</sub><sup>+</sup> (<sup>1</sup>Σ<sub>g</sub><sup>+</sup>). Since the IE's of Zn and NO<sub>2</sub> are similar, these two different charge states correspond to two low-lying potential-energy surfaces that couple as the Zn and NO<sub>2</sub> nuclei approach each other. There are other low-lying electronic states of NO<sub>2</sub>,<sup>59</sup> but these are unlikely to be important in the present problem and we ignore them for simplicity.

Since the equilibrium bond angle of neutral NO<sub>2</sub> is 134°, while that for NO<sub>2</sub><sup>+</sup> is 180°, it is important to consider the charge-transfer process as a function of both the O-N-O bond angle and the Zn-NO<sub>2</sub> reagent separation. Figure 4

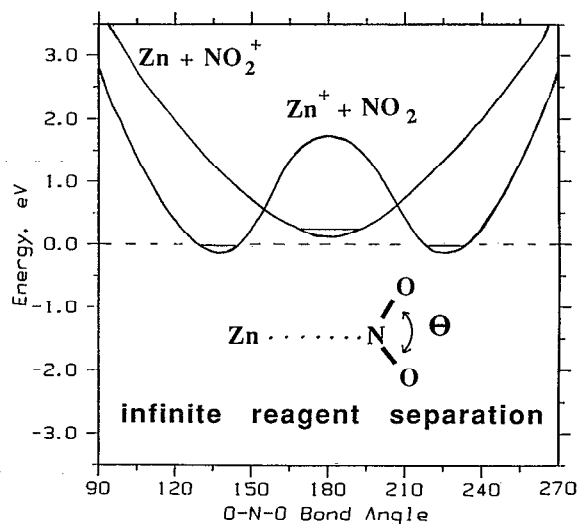


FIG. 4. Potential-energy diagrams as a function of the O-N-O bond angle for the Zn<sup>+</sup> + NO<sub>2</sub> and Zn + NO<sub>2</sub><sup>+</sup> charge states at infinite reagent separation.

shows the bending O–N–O coordinate of the potential surfaces for infinite Zn–NO<sub>2</sub> separation. These surfaces are the ground electronic surfaces of NO<sub>2</sub> and NO<sub>2</sub><sup>+</sup> offset by IE(Zn) such that the minima of the two surfaces are separated by 0.19 eV = IE(NO<sub>2</sub>) – IE(Zn). Since the energy of linear NO<sub>2</sub> neutral is ~1.8 eV (Refs. 59 and 60) higher in energy than bent NO<sub>2</sub>, the lowest-energy charge state is a function of the NO<sub>2</sub> angle, Fig. 4.

We now consider how these surfaces evolve as the Zn and NO<sub>2</sub> species approach. We assume that the most favorable approach is along the C<sub>2v</sub> symmetry axis of NO<sub>2</sub> since this geometry can lead to covalent bond formation between the radical electrons on Zn<sup>+</sup> and on NO<sub>2</sub>. Figure 5 shows qualitative one-dimensional potential-energy surfaces as a function of reagent separation for two fixed angles of NO<sub>2</sub>: 134° [Fig. 5(a)], as appropriate for neutral NO<sub>2</sub>, and 180° [Fig. 5(b)], as appropriate for ionic NO<sub>2</sub><sup>+</sup>. At both angles, the surfaces of both charge states should be attractive at long

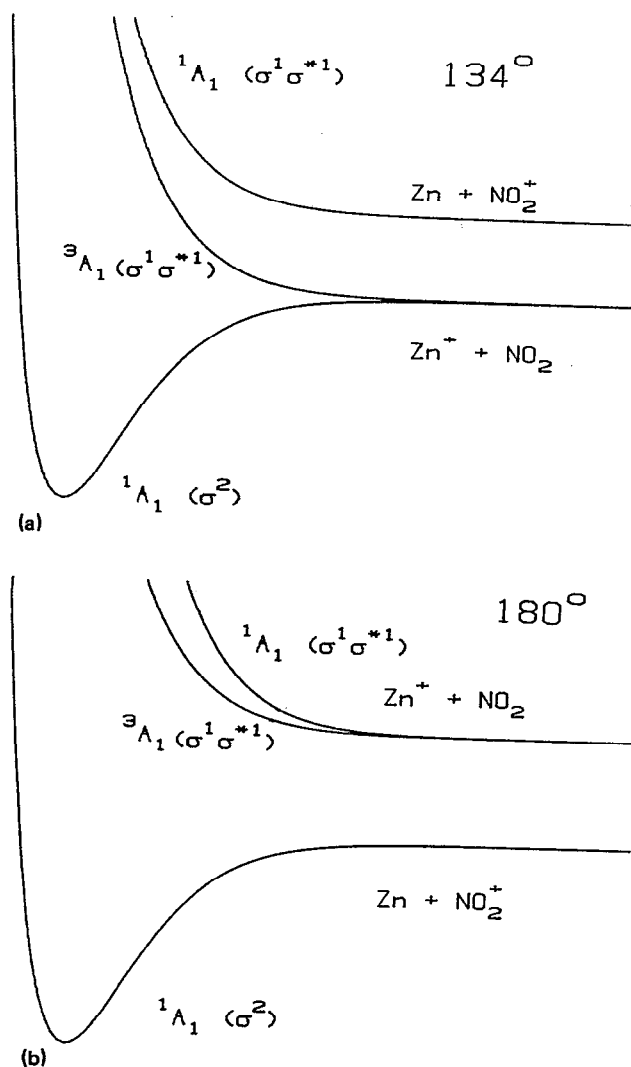


FIG. 5. Qualitative potential-energy surfaces for interaction of Zn<sup>+</sup> + NO<sub>2</sub> and Zn + NO<sub>2</sub><sup>+</sup> as a function of reagent separation at O–N–O bond angles fixed at (a) 134° and (b) 180°.

range due to ion-dipole and ion-induced dipole interactions. At 134°, Fig. 5(a), covalent bond formation between Zn<sup>+</sup> (<sup>2</sup>S) and NO<sub>2</sub> (<sup>2</sup>A<sub>1</sub>) should lead to a deep potential well along a <sup>1</sup>A<sub>1</sub>(σ<sup>2</sup>) surface (where σ is the molecular bonding orbital). We estimate the depth of this well to be ~3 eV, similar to the covalent bond energy for Zn<sup>+</sup>–CH<sub>3</sub> = 3.06 ± 0.16 eV.<sup>39</sup> Interaction of Zn<sup>+</sup> and NO<sub>2</sub> also forms a repulsive <sup>3</sup>A<sub>1</sub>(σ<sup>1</sup>σ\*<sup>1</sup>) surface (where σ\* is the molecular antibonding orbital). At 134°, interaction of Zn + NO<sub>2</sub><sup>+</sup> leads to a <sup>1</sup>A<sub>1</sub>(σ<sup>1</sup>σ\*<sup>1</sup>) surface that will be largely repulsive (except for long-range attractions).<sup>61</sup> When the O–N–O angle is fixed at 180°, Fig. 5(b), the same surfaces [one strongly attractive <sup>1</sup>A<sub>1</sub>(σ<sup>2</sup>) surface, one repulsive <sup>1</sup>A<sub>1</sub>(σ<sup>1</sup>σ\*<sup>1</sup>) surface, and one repulsive <sup>3</sup>A<sub>1</sub>(σ<sup>1</sup>σ\*<sup>1</sup>) surface] are formed, but now the strongly bound ZnNO<sub>2</sub><sup>+</sup> intermediate correlates adiabatically with the Zn + NO<sub>2</sub><sup>+</sup> charge state since it has the lowest asymptotic energy, Fig. 4.

A better understanding of the interaction that results between the two charge states can be obtained by combining the information in Figs. 4 and 5 to derive qualitative potential-energy surfaces as a function of both NO<sub>2</sub> bending coordinate and internuclear separation of the reagents. We do this by considering how Fig. 4 evolves as the nuclei get closer, Fig. 6, where only the singlet surfaces are shown. The first thing to note is that the symmetry associated with inversion of neutral NO<sub>2</sub> is broken due to the presence of the zinc atom. Thus, the energy of one of the NO<sub>2</sub> wells should be higher than the other, Fig. 6(a). As the nuclei approach further, the diabatic surfaces corresponding to the two charge states begin to mix since they both have <sup>1</sup>A<sub>1</sub> symmetry. This mixing between the surfaces increases as the distance between the reagents decreases, Figs. 6(a) and 6(b), and the crossing becomes avoided. In the region of the ground state of the ZnNO<sub>2</sub><sup>+</sup> complex, the splitting between the two adiabatic surfaces that have evolved, Figure 6(c), should be relatively large over a broad range of O–N–O bond angles.

The charge-transfer reaction of Zn<sup>+</sup> + NO<sub>2</sub> can be understood by considering the surfaces shown in Fig. 6 as the reagents approach one another to form a ZnNO<sub>2</sub><sup>+</sup> intermediate and as they separate to form products. At long ranges, Zn<sup>+</sup> approaches NO<sub>2</sub> with a bond angle near 134°. At closer range where the two charge state surfaces mix, the ZnNO<sub>2</sub><sup>+</sup> complex has an internal energy equivalent to D°(Zn<sup>+</sup> – NO<sub>2</sub>) plus the energy of the reagents. Therefore, this intermediate is free to vibrate on the attractive <sup>1</sup>A<sub>1</sub> potential-energy surface where it can sample a wide range of NO<sub>2</sub> bond angles, Fig. 6(c). As the Zn and NO<sub>2</sub> nuclei separate, the mixing between the surfaces lessens and the motion of the system becomes trapped on one of the diabatic charge-state surfaces. Figure 6 shows that the location of the electron depends on the NO<sub>2</sub> bond angle as the Zn and NO<sub>2</sub> separate. If the bond angle is near 180° when the coupling between the diabatic surfaces becomes weak, then the system proceeds to form Zn + NO<sub>2</sub><sup>+</sup>, while if the O–N–O bond angle is near 134°, there is a preference for returning to reactants, Zn<sup>+</sup> + NO<sub>2</sub>.

For a reaction involving NO<sup>+</sup>, the situation changes somewhat in that the reaction is now more endothermic and

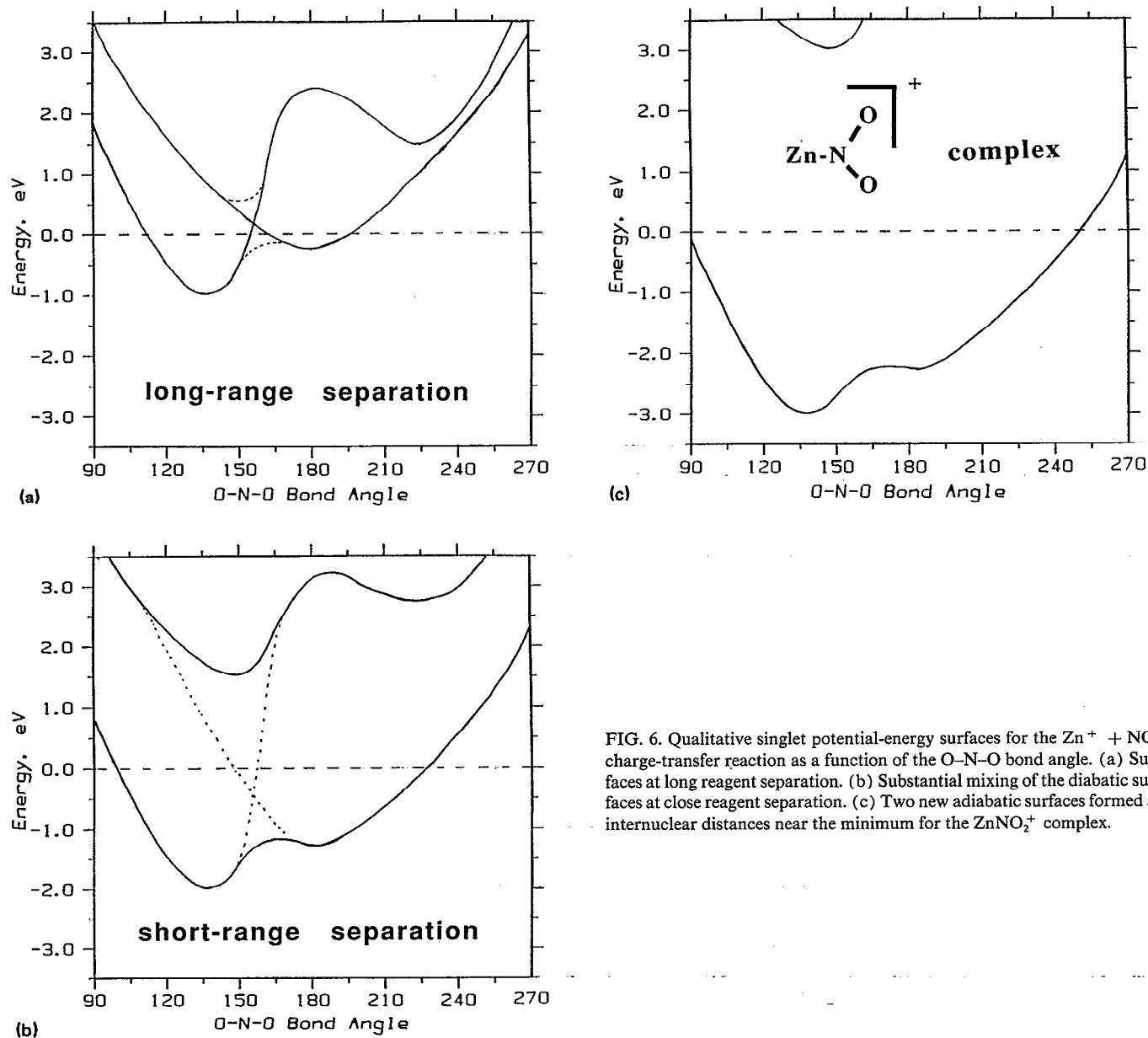


FIG. 6. Qualitative singlet potential-energy surfaces for the  $\text{Zn}^+ + \text{NO}_2$  charge-transfer reaction as a function of the O-N-O bond angle. (a) Surfaces at long reagent separation. (b) Substantial mixing of the diabatic surfaces at close reagent separation. (c) Two new adiabatic surfaces formed at internuclear distances near the minimum for the  $\text{ZnNO}_2^+$  complex.

NO<sup>+</sup> has a  $^1\Sigma^+$  ground state. Thus, no covalent two-electron bond can be formed between NO<sup>+</sup> and NO<sub>2</sub>, although the radical electron that is transferred between these species can form a one-electron two-center bond. Overall, the stability of the NO<sup>+</sup>-NO<sub>2</sub> intermediate is expected to be less than that for Zn<sup>+</sup>-NO<sub>2</sub>. This combined with the increased endothermicity may decrease the degree of mixing between the two charge state surfaces. This may explain why the cross section for reaction (9) rises less rapidly from threshold than that for reaction (8), Fig. 3, an indication that this reaction is less efficient than in the zinc system.

The net result of this ionization mechanism is that the NO<sub>2</sub> bond angle can easily adjust to minimize the energy during the electron transfer process. Since the agent for inducing ionization is the heavy Zn<sup>+</sup> or NO<sup>+</sup> ion, rather than a photon or electron, the time scale for loss of the electron is

directly comparable to the timescale for nuclear motion. Thus, the Franck-Condon limitations on vertical processes are not exhibited in these reaction systems. This result does not necessarily hold for off-resonance charge-transfer reactions. Here, the transition-state intermediates need not be as intimate or as long lived. Thus, the nuclear motion of the system may not control the ionization process and a vertical ionization process may be observed.<sup>62</sup>

#### ACKNOWLEDGMENTS

This work is supported by the National Science Foundation, Grant No. CHE-8917980. We are also grateful for the ideas of Edward Earl and Professor Jack Simons about generation of the qualitative potential-energy surfaces.

- <sup>1</sup> E. C. G. Stuecklberg and H. D. Smyth, *Phys. Rev.* **36**, 478 (1930).
- <sup>2</sup> R. J. Kandell, *J. Chem. Phys.* **23**, 84 (1955).
- <sup>3</sup> J. Collin and F. P. Lossing, *J. Chem. Phys.* **28**, 900 (1958).
- <sup>4</sup> R. W. Kiser and I. C. Hisatsune, *J. Phys. Chem.* **65**, 1444 (1961).
- <sup>5</sup> J. E. Collin, *Nature* **196**, 373 (1962).
- <sup>6</sup> S. Tsuda and W. H. Hamill, *Adv. Mass Spectrom.* **3**, 249 (1966).
- <sup>7</sup> K. Stephan, H. Helm, Y. B. Kim, G. Seykora, J. Ramlar, and M. Grossl, *J. Chem. Phys.* **73**, 303 (1980).
- <sup>8</sup> G. L. Weisler, J. A. R. Samson, M. Ogawa, and G. R. Cook, *J. Opt. Soc. Am.* **49**, 338 (1959).
- <sup>9</sup> T. Nakayama, M. Y. Kitamura, and K. Watanabe, *J. Chem. Phys.* **30**, 1180 (1959).
- <sup>10</sup> D. C. Frost, D. Mak, and C. A. McDowell, *Can. J. Chem.* **40**, 1064 (1962).
- <sup>11</sup> V. H. Dibeler, J. A. Walker, and S. K. Liston, *J. Res. Natl. Bur. Stand. (U.S.)* **71**, 371 (1967), as cited in Ref. 14.
- <sup>12</sup> P. C. Killgoar, Jr., G. E. Leroi, W. A. Chupka, and J. Berkowitz, *J. Chem. Phys.* **59**, 1370 (1973).
- <sup>13</sup> C. R. Brundle, D. Neumann, W. C. Price, D. Evans, A. W. Potts, and D. G. Streets, *J. Chem. Phys.* **53**, 705 (1970); C. R. Brundle, *Chem. Phys. Lett.* **5**, 140 (1970).
- <sup>14</sup> P. Natalis and J. E. Collin, *Chem. Phys. Lett.* **2**, 79 (1968).
- <sup>15</sup> O. Edqvist, E. Lindholm, L. E. Selin, L. Asbrink, C. E. Küyatt, S. R. Mielczarek, J. A. Simpson, and I. Fischer-Hjalmers, *Phys. Scr.* **1**, 172 (1970).
- <sup>16</sup> P. Natalis, J. Delwiche, and J. E. Collin, *Chem. Phys. Lett.* **9**, 139 (1971).
- <sup>17</sup> M. I. Al-Joboury, Ph. D. thesis, University of British Columbia, Vancouver, 1966, as cited in Ref. 14.
- <sup>18</sup> W. C. Price and D. M. Simpson, *Trans. Faraday Soc.* **37**, 106 (1941).
- <sup>19</sup> Y. Tanaka and A. S. Jursa, *J. Chem. Phys.* **36**, 2493 (1962).
- <sup>20</sup> K. S. Haber, J. W. Zwanziger, F. X. Campos, R. T. Wiedmann, and E. R. Grant, *J. Chem. Phys.* **144**, 58 (1988).
- <sup>21</sup> F. C. Fehsenfeld, E. E. Ferguson, and M. Mosesman, *Chem. Phys. Lett.* **4**, 73 (1969).
- <sup>22</sup> P. Ausloos and S. G. Lias, *Int. J. Chem. Kin.* **X**, 657 (1978).
- <sup>23</sup> G. Herzberg, *Electronic Spectra and Electronic Structure of Polyatomic Molecules* (Van Nostrand, Princeton, New Jersey, 1967).
- <sup>24</sup> K. Kimura, S. Katsumata, Y. Achiba, T. Yamazaki, and S. Iwata, *Handbook of HeI Photoelectron Spectra of Fundamental Organic Molecules* (Japan Scientific Societies Press, New York, 1981).
- <sup>25</sup> S. G. Lias, J. E. Bartmess, J. F. Liebman, J. L. Holmes, R. D. Levin, and W. G. Mallard, *J. Phys. Chem. Ref. Data* **17**, Suppl. 1 (1988).
- <sup>26</sup> Y. Tanaka and A. S. Jursa, *J. Chem. Phys.* **36**, 2493 (1962).
- <sup>27</sup> D. L. Baulch, R. A. Cox, P. J. Crutzen, R. F. Hampson, Jr., J. A. Kerr, J. Troe, and R. T. Watson, *J. Phys. Chem. Ref. Data* **11**, 327 (1982).
- <sup>28</sup> R. S. Tapper, R. L. Whetten, G. S. Ezra, and E. R. Grant, *J. Phys. Chem.* **88** (1984) 1273.
- <sup>29</sup> L. Bigio and E. R. Grant, *J. Chem. Phys.* **83**, 5361 (1985).
- <sup>30</sup> K. M. Ervin and P. B. Armentrout, *J. Chem. Phys.* **83**, 166 (1985).
- <sup>31</sup> All neutral gases were purified before use. NO<sub>2</sub> was obtained from Matheson in 99.5% purity and was subjected to multiple freeze-pump-thaw cycles using liquid nitrogen. During the first freeze cycle, the solid phase (N<sub>2</sub>O<sub>4</sub>) was always a blue-green color indicating that N<sub>2</sub>O<sub>3</sub> was also present. Before thawing, an excess of oxygen gas (roughly 10 to 20 times more than the initial NO<sub>2</sub> added) was introduced to the system. The frozen nitrogen oxides were allowed to warm up in the excess of oxygen such that any NO formed from decomposition of N<sub>2</sub>O<sub>3</sub> reacted with oxygen to form NO<sub>2</sub>. Upon refreezing the resulting NO<sub>2</sub> and oxygen mixture, the resulting solid phase was always a white powder with a slight yellow tint (indicating that N<sub>2</sub>O<sub>4</sub> was the main species). The excess oxygen was pumped away while the N<sub>2</sub>O<sub>4</sub> was held at liquid-nitrogen temperatures. Pressures in the bulb were kept below ~50 Torr, in order to favor NO<sub>2</sub> in the 2NO<sub>2</sub> = N<sub>2</sub>O<sub>4</sub> equilibrium.  $\alpha,\alpha,\alpha$ -trifluorotoluene was obtained from Fluka (99%) and was subjected to multiple freeze-pump-thaw cycles to remove any gaseous contaminants.
- <sup>32</sup> P. J. Chantry, *J. Chem. Phys.* **55**, 2746 (1971).
- <sup>33</sup> Doppler broadening widths for the systems studied here are 0.34, 0.41, 0.26, 0.27, and 0.47 times  $E^{1/2}$  for the NO<sup>+</sup> + NO<sub>2</sub>, Zn<sup>+</sup> + NO<sub>2</sub>, NO<sub>2</sub><sup>+</sup> + C<sub>6</sub>H<sub>5</sub>CF<sub>3</sub>, NO<sub>2</sub><sup>+</sup> + CH<sub>3</sub>I, and CH<sub>3</sub>I<sup>+</sup> + NO<sub>2</sub> systems, respectively.
- <sup>34</sup> For a complete description of this source, see R. H. Schultz and P. B. Armentrout, *Int. J. Mass Spectrom. Ion Processes*, **95**, 121 (1991).
- <sup>35</sup> R. H. Schultz, K. C. Crellin, and P. B. Armentrout, *J. Am. Chem. Soc.* **113**, 8590 (1991).
- <sup>36</sup> E. R. Fisher, B. L. Kickel, and P. B. Armentrout (unpublished).
- <sup>37</sup> E. R. Fisher, B. L. Kickel, and P. B. Armentrout (unpublished).
- <sup>38</sup> Using electron impact ionization with electron energies below 15 eV ensures that only Zn<sup>+</sup> (<sup>2</sup>S) is formed since IE(Zn) = 9.394 eV, and the first excited state of Zn<sup>+</sup> lies 6.01 eV higher in energy.
- <sup>39</sup> R. Georgiadis and P. B. Armentrout, *J. Am. Chem. Soc.* **108**, 2119 (1986).
- <sup>40</sup> E. R. Fisher and P. B. Armentrout, *J. Chem. Phys.* **94**, 1150 (1991).
- <sup>41</sup> R. H. Schultz and P. B. Armentrout, *Chem. Phys. Lett.* **179**, 429 (1991).
- <sup>42</sup> R. H. Schultz and P. B. Armentrout, *J. Chem. Phys.* **95**, 121 (1991).
- <sup>43</sup> T. Baer, W. B. Peatman, and E. W. Schlag, *Chem. Phys. Lett.* **4**, 243 (1969).
- <sup>44</sup> The vibrational frequencies of NO<sub>2</sub><sup>+</sup> for the symmetric stretch ( $\nu_1 = 1404$ ) and bend ( $\nu_2 = 614.5$  cm<sup>-1</sup>) are assumed to be the same as those given in Ref. 28 and for the linear Rydberg state. The asymmetric stretching frequency  $\nu_3 = 2349$  cm<sup>-1</sup> is estimated as the value for that stretch found in CO<sub>2</sub> which is isoelectronic with NO<sub>2</sub><sup>+</sup>.
- <sup>45</sup> S. G. Lias and P. Ausloos, *J. Am. Chem. Soc.* **100**, 6027 (1978).
- <sup>46</sup> N. Aristov and P. B. Armentrout, *J. Am. Chem. Soc.* **108**, 1806 (1986).
- <sup>47</sup> W. J. Chesnavich and M. T. Bowers, *J. Phys. Chem.* **83**, 900 (1979).
- <sup>48</sup> L. Sunderlin, N. Aristov, and P. B. Armentrout, *J. Am. Chem. Soc.* **109**, 78 (1987).
- <sup>49</sup> P. B. Armentrout and J. L. Beauchamp, *J. Chem. Phys.* **74**, 2819 (1981); *J. Am. Chem. Soc.* **103**, 784 (1981).
- <sup>50</sup> B. H. Boo and P. B. Armentrout, *J. Am. Chem. Soc.* **109**, 3549 (1987).
- <sup>51</sup> P. B. Armentrout, in *Advances in Gas Phase Ion Chemistry, Vol. 1*, edited by N. G. Adams and L. M. Babcock (JAI Press, Greenwich, Connecticut, 19XX).
- <sup>52</sup> T. Beyer and D. F. Swinehart, *Comm. Assoc. Comput. Machines* **16**, 379 (1973); S. E. Stein and B. S. Rabinovitch, *J. Chem. Phys.* **58**, 2438 (1973); *Chem. Phys. Lett.* **49**, 183 (1977); R. G. Gilbert and S. C. Smith, *Theory of Unimolecular and Recombination Reactions* (Blackwell Scientific, Oxford, 1990).
- <sup>53</sup> G. Gioumousis and D. P. Stevenson, *J. Chem. Phys.* **29**, 292 (1958).
- <sup>54</sup> The collision cross section for the LGS model is given by  $\sigma_{LGS} = \pi e(2\alpha/E)^{1/2}$ . We assume that  $\alpha(C_7H_5F_3) \approx 12.8 \text{ \AA}^3$ , taken as the sum of the polarizabilities for benzene ( $\alpha = 9.99 \text{ \AA}^3$ ) and CF<sub>3</sub>, estimated to be equivalent to  $\alpha(HCF_3) = 2.77 \text{ \AA}^3$ . This estimated polarizability yields  $\sigma_{LGS} = 250 \text{ \AA}^2$  at 0.06 eV.
- <sup>55</sup> The collision cross section for the locked-dipole model is  $\sigma_{LD} = 2\pi e[(\alpha/2E)^{1/2} + \mu/2E]$ , [T. F. Moran and W. H. Hamill, *J. Chem. Phys.* **39**, 1413 (1963)]. The polarizability is  $\alpha(CH_3I) = 7.29 \text{ \AA}^3$  and the dipole moment is  $\mu(CH_3I) = 1.65$  D [E. W. Rothe and R. B. Bernstein, *J. Chem. Phys.* **31**, 1619 (1959)].
- <sup>56</sup> T. Baer, W. B. Peatman, and E. W. Schlag, *Chem. Phys. Lett.* **4**, 243 (1969).
- <sup>57</sup> C. M. Brown, S. G. Tilford, and M. L. Ginter, *J. Opt. Soc. Am.* **65**, 1404 (1975).
- <sup>58</sup> For a complete discussion of the Zn<sup>+</sup> + NO<sub>2</sub> system, see D. E. Clemmer, N. F. Dalleska, and P. B. Armentrout, *J. Chem. Phys.* **95**, 7263 (1991).
- <sup>59</sup> G. D. Gillespie and A. U. Khan, *J. Chem. Phys.* **65**, 1624 (1976).
- <sup>60</sup> J. L. Hardwick and J. C. D. Brand, *Chem. Phys. Lett.* **21**, 458 (1973).
- <sup>61</sup> P. B. Armentrout and J. Simons (unpublished).
- <sup>62</sup> E. R. Fisher and P. B. Armentrout, *J. Chem. Phys.* **93**, 4858 (1990).